Technical note: Analytical sensitivity analysis and uncertainty estimation of a two-component hydrograph separation method which uses conductivity as a tracer

Weifei Yang[1], Changlai Xiao[1], Xiujuan Liang[1]

5   1 Key Laboratory of Groundwater Resources and Environment, Ministry of Education, and National-Local Joint Engineering Laboratory of In-situ Conversion, Drilling and Exploitation Technology for Oil Shale, and College of New Energy and Environment, Jilin University, No 2519, Jiefang Road, Changchun 130021, PR China

Correspondence to: Changlai Xiao (xcl2822@126.com, jluywf@126.com)

Abstract. The conductivity two-component hydrograph separation method is cheap and easy to operate and is favored by

10   hydrologists. This paper analyzes the sensitivity of the baseflow index (BFI, the long-term ratio of baseflow to streamflow) calculated by this method to errors or uncertainties of the two parameters (BF_C, the conductivity of baseflow; RO_C, the conductivity of surface runoff) and of the two variables (y_k, the specific streamflow; Q_{ck}, the specific conductivity of streamflow), and then estimates the uncertainty of BFI. The analysis shows that when the time series is longer than 365 days, the random measurement errors of y_k or Q_{ck} will cancel each other, and the influence on BFI can be neglected. Dimensionless

15   sensitivity indices (the ratio of the relative error of BFI to the relative error of BF_C or RO_C) can well express the propagation of errors or uncertainties of BF_C or RO_C into BFI. Based on the sensitivity analysis, the uncertainty estimation method of BFI is derived. Representative sensitivity indices and BFI' uncertainties are yielded by application of the resulting equations to 24 watersheds in the United States. The results indicate that BFI is more sensitive to BF_C, and the conductivity two-component hydrograph separation method may be more suitable for the long time series in a small watershed. After considering the mutual

20   offset of the measurement errors of conductivity and streamflow, the uncertainty of BFI is reduced by half.

1 Introduction

Hydrograph separation (also called baseflow separation), can effectively identify the proportion of water in different runoff pathways in a basin's export flow, which helps to identify the conversion relationship between groundwater and surface water, and is a necessary condition for optimal allocation of water resources (Cartwright et al., 2014; Miller et al., 2014; Costelloe et al.,

25   2015). Chemical/isotope (tracer) hydrograph separation method is considered to be the most effective separation method, which can reflect the actual characteristics of a basin (Mei and Anagnostou, 2015; Zhang et al., 2017). Many hydrologists have indicated that electrical conductivity can be used as a tracer to perform hydrograph separation (Stewart et al., 2007; Munyaneza et al., 2012; Cartwright et al., 2014; Lott and Stewart, 2016; Okello et al., 2018). The measurement of conductivity is simple and inexpensive and has a distinct applicability in a long series of hydrograph separation (Okello et al., 2018).

30   The conductivity two-component hydrograph separation method (also called conductivity mass balance method (CMB) (Stewart et al. 2007)) uses conductivity as a tracer to calculate baseflow through a two-component mass balance equation. The general equation is shown in Eq. (1).

$$b_k = \frac{y_k(Q_{ck} - RO_C)}{BF_C - RO_C} \tag{1}$$

where b is the baseflow (L^3/t), y is the streamflow (L^3/t), Q_c is the electrical conductivity of streamflow, and k is the time step

35   number. The two parameters BF_C and RO_C respectively represent the electrical conductivity of baseflow and surface runoff.

The field test of Stewart et al. (2007) showed that the maximum conductivity of streamflow can be used to replace BF_C, and the minimum conductivity can be used to replace RO_C. However, Miller et al. (2014) pointed out that the maximum conductivity of streamflow may exceed the real BF_C, so they suggested that the 99th percentile of the conductivity of a long series of streamflow should be used as the BF_C to avoid the impact of high BF_C estimates on the separation results. There is uncertainty in

5   determining the parameters (BF_C, RO_C) of the conductivity two-component hydrograph separation method (Miller et al., 2014; Okello et al., 2018). The sensitivity analysis of parameters and the uncertainty quantitative analysis of separation results are helpful to further optimize the conductivity two-component hydrograph separation method and improve the accuracy of hydrograph separation.

Most of the existing parameter sensitivity analysis methods use experimental sensitivity analysis method, which usually

10   substitutes the fluctuation value of a certain parameter into the separation model, and then analyzes the sensitivity of the parameters by comparing the range of the separation results produced by these fluctuation parameters (Eckhradt, 2005; Miller et al., 2014; Okello et al., 2018). Eckhardt (2012) indicated that "An empirical sensitivity analysis is only an analytical calculation of the error propagation through the model, is not feasible." Eckhardt (2012) derived the sensitivity indices of the equation parameters by the partial derivative of a two-parameter recursive digital baseflow separation filter equation. However, the

15   parameters' sensitivity indices of the conductivity two-component hydrograph separation equation have not been derived.

At present, the uncertainty of the separation results of the conductivity two-component hydrograph separation method is mainly estimated by uncertainty transfer equation based on the uncertainty of BF_C, RO_C, and Q_{ck} (Genereux, 1998; Miller et al., 2014). See Sect. 3.1 for details. This method can only estimate the uncertainty of the baseflow ratio (f_{bf}, the ratio of baseflow to streamflow in a single calculation process), and then use the average uncertainty of multiple calculation processes to estimate the

20   uncertainty of the baseflow index (BFI, the long-term ratio of baseflow to total streamflow). This uncertainty estimation method can neither directly estimate the uncertainty of BFI nor consider the randomness and mutual offset of conductivity measurement error, and the uncertainty estimation of BFI is not appropriate enough.

The purpose of this paper is to derive the parameters' sensitivity indices of the conductivity two-component hydrograph separation equation by calculating the partial derivative of Eq. (1) (Sect. 2), and further derive the direct estimation method of

25   BFI' uncertainty (Sect. 3). The derived methods were applied to 24 basins in the United States, and the parameters' sensitivity indices and BFI' uncertainty characteristics were analyzed (Sect. 4).

2 Analytical sensitivity analysis

2.1 Parameters BF_C and RO_C

In order to calculate the sensitivity indices of the parameters, the partial derivatives of b_k in Eq. (1) to BF_C and RO_C are required

30   respectively (for the derivation process, see Appendix A1, A2):

$$\frac{\partial b_k}{\partial BF_C} = -y_k \frac{Q_{ck} - RO_C}{(BF_C - RO_C)^2} \tag{2}$$

$$\frac{\partial b_k}{\partial RO_C} = y_k \frac{Q_{ck} - BF_C}{(BF_C - RO_C)^2} \tag{3}$$

For the convenience of comparison, the baseflow index (BFI) is selected as the baseflow separation result for long time series to analyze the influence of parameters' uncertainty on BFI,

35    $$BFI = \frac{\sum_{k=1}^{n} b_k}{\sum_{k=1}^{n} y_k} = \frac{b}{y} \tag{4}$$

where b denotes the total baseflow and y the total streamflow over the whole available streamflow sequences, n is the number of available streamflow data.

Then, the partial derivatives of BFI to BF_C and RO_C should be calculated, (for the derivation process, see Appendix A3, A4):

$$\frac{\partial \text{BFI}}{\partial \text{BF}_c} = \frac{y\text{RO}_c - \sum_{k=1}^{n} y_k Q_{ck}}{y(\text{BF}_c - \text{RO}_c)^2} \tag{5}$$

$$\frac{\partial \text{BFI}}{\partial \text{RO}_c} = \frac{\sum_{k=1}^{n} y_k Q_{ck} - y\text{BF}_c}{y(\text{BF}_c - \text{RO}_c)^2} \tag{6}$$

It can be seen from the definition of the partial derivative that the influence of the errors of the parameters (ΔBF_C and ΔRO_C) in

Eq. (1) on the BFI can be expressed by the product of the errors and its partial derivatives. Then the BFI' errors caused by tiny

errors of BF_C and RO_C can be expressed as:

$$\Delta_{\text{BF}_c}\text{BFI} = \frac{\partial \text{BFI}}{\partial \text{BF}_c}\Delta \text{BF}_c = \frac{y\text{RO}_c - \sum_{k=1}^{n} y_k Q_{ck}}{y(\text{BF}_c - \text{RO}_c)^2}\Delta \text{BF}_c \tag{7}$$

$$\Delta_{\text{RO}_c}\text{BFI} = \frac{\partial \text{BFI}}{\partial \text{RO}_c}\Delta \text{RO}_c = \frac{\sum_{k=1}^{n} y_k Q_{ck} - y\text{BF}_c}{y(\text{BF}_c - \text{RO}_c)^2}\Delta \text{RO}_c \tag{8}$$

The dimensionless sensitivity indices (S) can be obtained by comparing the relative error of BFI caused by the tiny errors of BF_C

and RO_C with that of BF_C and RO_C, (see Appendix B1, B2):

$$S(\text{BFI}/\text{BF}_c) = \frac{\Delta_{\text{BF}_c}\text{BFI}}{\text{BFI}} \Big/ \frac{\Delta \text{BF}_c}{\text{BF}_c} = \frac{\text{BF}_c(y\text{RO}_c - \sum_{k=1}^{n} y_k Q_{ck})}{y\text{BFI}(\text{BF}_c - \text{RO}_c)^2} \tag{9}$$

$$S(\text{BFI}/\text{RO}_c) = \frac{\Delta_{\text{RO}_c}\text{BFI}}{\text{BFI}} \Big/ \frac{\Delta \text{RO}_c}{\text{RO}_c} = \frac{\text{RO}_c(\sum_{k=1}^{n} y_k Q_{ck} - y\text{BF}_c)}{y\text{BFI}(\text{BF}_c - \text{RO}_c)^2} \tag{10}$$

where $S(\text{BFI}/\text{BF}_c)$ represent the dimensionless sensitivity index of BFI (output) with BF_c (uncertain input), and $S(\text{BFI}/\text{RO}_c)$

with RO_c.

The dimensionless sensitivity index is also called "elasticity index", it reflects the proportional relationship between the relative

error of BFI and the relative error of parameters (e.g. $S(\text{BFI}/\text{BF}_c) = 1.5$, the relative error of BF_c is 5%, then the relative error of

BFI should be 1.5 times 5% (7.5%)). After determining the specific values of BF_C, RO_C, BFI, y, y_k and Q_{ck}, the sensitivity indices

$S(\text{BFI}/\text{BF}_c)$ and $S(\text{BFI}/\text{RO}_c)$ can be calculated and compared.

2.2 Variables y_k and Q_{ck}

In addition to the two parameters, there are two variables (Q_{ck} and y_k) in Eq. (1). This section will analyze the sensitivity of BFI

to these two variables. Similar to Sect. 2.1, the partial derivatives of b_k in Eq. (1) to Q_{ck} and y_k are obtained (see Appendix A5,

A6), and the partial derivatives of BFI to Q_{ck} and y_k are further obtained (see Appendix A7, A8),

$$\frac{\partial \text{BFI}}{\partial Q_{ck}} = \frac{1}{\text{BF}_c - \text{RO}_c} \tag{11}$$

$$\frac{\partial \text{BFI}}{\partial y_k} = \frac{\sum_{k=1}^{n}(Q_{ck} - \text{RO}_c) - \text{BFI}(\text{BF}_c - \text{RO}_c)}{y(\text{BF}_c - \text{RO}_c)} \tag{12}$$

According to previous studies (Munyaneza et al., 2012; Cartwright et al., 2014; Miller et al., 2014; Okello et al., 2018) and this

study (Table 1), the difference between BF_C and RO_C is often greater than 100 μs/cm, so $\partial \text{BFI}/\partial Q_{ck}$ is usually less than 0.01.

Appendix C shows that the value of $\partial \text{BFI}/\partial y_k$ is usually far less than 1.

Tiny errors in Q_{ck} and y_k cause errors in BFI of

$$\Delta_{Q_{ck}}\text{BFI} = \frac{\partial \text{BFI}}{\partial Q_{ck}}\Delta Q_{ck} = \frac{\Delta Q_{ck}}{\text{BF}_c - \text{RO}_c} \tag{13}$$

$$\Delta_{y_k}\text{BFI} = \frac{\partial \text{BFI}}{\partial y_k}\Delta y_k = \frac{\sum_{k=1}^{n}(Q_{ck} - \text{RO}_c) - \text{BFI}(\text{BF}_c - \text{RO}_c)}{y(\text{BF}_c - \text{RO}_c)}\Delta y_k \tag{14}$$

The errors of BFI caused by Q_{ck} and y_k are summed up to get the error of BFI caused by $\sum_{k=1}^{n} Q_{ck}$ and $\sum_{k=1}^{n} y_k$ in the whole time

series:

$$\Delta_{\sum_{k=1}^{n} Q_{ck}}\text{BFI} = \sum_{k=1}^{n}\Delta_{Q_{ck}}\text{BFI} = \sum_{k=1}^{n}\frac{\Delta Q_{ck}}{\text{BF}_c - \text{RO}_c} = \frac{1}{\text{BF}_c - \text{RO}_c}\sum_{k=1}^{n}\Delta Q_{ck} \tag{15}$$

$$\Delta_{\sum_{k=1}^{n} y_k} \text{BFI} = \sum_{k=1}^{n} \Delta_{y_k} \text{BFI} = \sum_{k=1}^{n} \left(\frac{\sum_{k=1}^{n}(Q_{ck}-\text{RO}_c)-\text{BFI}(\text{BF}_c-\text{RO}_c)}{y(\text{BF}_c-\text{RO}_c)} \Delta y_k \right) = \frac{\sum_{k=1}^{n}(Q_{ck}-\text{RO}_c)-\text{BFI}(\text{BF}_c-\text{RO}_c)}{y(\text{BF}_c-\text{RO}_c)} \sum_{k=1}^{n} \Delta y_k \qquad (16)$$

The tiny errors in Q_{ck} and y_k are mainly composed of random analysis errors. Random errors mostly follow a normal distribution or a uniform distribution. The magnitude and direction of the random errors are usually not fixed. As the number of measurements increases, the positive and negative errors can compensate each other, and the average value of the errors will gradually trend to zero (Huang and Chen, 2011).

The uncertainty of the instruments is <5% for Q_{ck} less than 100 μs/cm and <3% for Q_{ck} greater than 100 μs/cm (Wagner et al., 2006; Miller et al., 2014). The measurement uncertainty of streamflow is usually <3% (Zhang, 2005). In this paper, the error ranges of Q_{ck} and y_k are considered to be ±5% and ±3%, respectively. Considering the mutual offset of random errors, when the time series (n) is long enough, $\sum_{k=1}^{n} \Delta Q_{ck}$ in Eq. (15) and $\sum_{k=1}^{n} \Delta y_k$ in Eq. (16) will approach zero. Therefore, when n is large enough, the error of BFI caused by the errors of Q_{ck} and y_k can be neglected.

To verify this phenomenon, the study collected the daily average conductivity and daily average streamflow of the surface water station with the USGS site number 0297100 (Table 1) from 2001 to 2010 (2979 days in total). Then, office Excel was used to generate 10 sets (2979 per set) of random numbers between -0.05 and 0.05 that obey normal distribution and uniform distribution respectively to simulate the errors (%) of the daily average conductivity. And 10 sets (2979 per set) of random numbers obeying normal distribution and uniform distribution between -0.03 and 0.03, respectively, were used to simulate the errors (%) of the daily average streamflow. Finally, according to different time series (n) (e.g. 30, 60, 90, 120, 150, 180, 210, 240, 270, 300, 365, 730, 1095, … , 2979, days) sum the errors value ($\sum_{k=1}^{n} \Delta Q_{ck}$ and $\sum_{k=1}^{n} \Delta y_k$) and analyze the trend of the average error (%) with n.

The trend of the average error (%) of conductivity with n is shown in Fig. 1. The average errors of the uniform distribution (Fig. 1(a)) and the normal distribution (Fig. 1(b)) are all gradually approach zero with the increase of the time series (n), and the uniform distribution converges faster than the normal distribution. The average errors of the two distributions are between -2% and 2%, and the absolute value of the average errors are less than 0.49% when n is greater than 365.

Similar to the conductivity, the trend of the average error (%) of the streamflow with n is shown in Fig. 2. The average errors of the uniform distribution (Fig. 2(a)) and the normal distribution (Fig. 2(b)) all gradually approach to zero as the time series (n) increases, and the uniform distribution converges faster than the normal distribution. The average errors of different n under the two distributions are between -2% and 2%, and the absolute value of the average errors are less than 0.67% when n is greater than 365.

From the above analysis, when the time series (n) is greater than 365 days (1 year), $\Delta_{\sum_{k=1}^{n} Q_{ck}} \text{BFI}$ will be less than 0.0049% (0.01 times 0.49%), and $\Delta_{\sum_{k=1}^{n} y_k} \text{BFI}$ will be much less than 0.76% (1 times 0.76%). Therefore, the random errors of daily average conductivity and streamflow have a negligible effect on BFI.

Figure 1. Average conductivity error (%) with different distributions along the time series (n), (a) uniform distribution, (b) normal distribution.

Figure 2. Average streamflow error (%) with different distributions along the time series (n), (a) uniform distribution, (b) normal distribution.

3 Uncertainty estimation

3.1 Previous attempts

According to previous studies, in the case where a parameter g is calculated as a function of several factors $x_1, x_2, x_3, ..., x_n$ (e.g. g= G($x_1, x_2, x_3, ..., x_n$)). The transfer equation between the uncertainty of the independent factors and the uncertainty of g is

5 (Taylor, 1982; Kline, 1985; Genereux, 1998):

$$W_g = \sqrt{(\frac{\partial g}{\partial x_1} W_{x_1})^2 + (\frac{\partial g}{\partial x_2} W_{x_2})^2 + \cdots + (\frac{\partial g}{\partial x_n} W_{x_n})^2} \qquad (17)$$

where W_g, W_{x_1}, W_{x_2}, and W_{xn} are the same type of uncertainty values (e.g. all average errors or all standard deviations) for g, x_1, x_2, and x_n, respectively.

Based on the above principle, Genereux (1998) substituted Eq. (18) into Eq. (17) to derive the uncertainty estimation equation

10 (Eq. (19)) of the two-component mass balance baseflow separation method:

$$f_{bf} = \frac{Q_{ck} - RO_c}{BF_c - RO_c} \qquad (18)$$

$$W_{f_{bf}} = \sqrt{(\frac{f_{bf}}{BF_c - RO_c} W_{BF_C})^2 + (\frac{1 - f_{bf}}{BF_c - RO_c} W_{RO_c})^2 + (\frac{1}{BF_c - RO_c} W_{Q_c})^2} \qquad (19)$$

where f_{bf} is the ratio of baseflow to streamflow in a single calculation process, W_{fbf} is the uncertainty in f_{bf} at the 95% confidence interval, W_{BFC} is the standard deviation of the highest 1% of measured conductivity multiplied by the t-value (α=0.05; two-tail) from the Student's distribution, W_{ROC} is the standard deviation of the lowest 1% of measured conductivity multiplied by the t-value (α=0.05; two-tail) from the Student's distribution, and W_{QC} is the analytical error in the conductivity multiplied by the t-value (α=0.05; two-tail) (Miller et al., 2014).

Equation (19) can better estimate the uncertainty of f_{bf} within a single calculation step. Hydrologists usually estimate the uncertainty of BFI approximately by averaging the uncertainty of all steps (Genereux, 1998; Miller et al., 2014). However, this

20 method does not consider the mutual offset of the conductivity measurement errors, and cannot accurately reflect the uncertainty of BFI. In this paper, based on the parameter sensitivity analysis, the uncertainty estimation equation of BFI is derived. See the next section for details.

3.2 Uncertainty estimation in BFI

BFI is a function of BF_c, RO_c, Q_{ck} and y_k. And the uncertainty of BF_c, RO_c, Q_{ck} and y_k is independent of each other. Sect. 2.2

25 has explained that the random errors of daily average conductivity and streamflow have a negligible effect on BFI when the time series (n) is greater than 365 days (1 year), so the uncertainty of BFI can be expressed as:

$$W_{BFI} = \sqrt{(\frac{\partial BFI}{\partial BF_c} W_{BF_C})^2 + (\frac{\partial BFI}{\partial RO_c} W_{RO_C})^2} \qquad (20)$$

where (see Eq. 5 and Eq. 9; Eq. 6 and Eq. 10)

$$\frac{\partial BFI}{\partial BF_c} = S(BFI/BF_c) \frac{BFI}{BF_c} \qquad (21)$$

30 $$\frac{\partial BFI}{\partial RO_c} = S(BFI/RO_c) \frac{BFI}{RO_c} \qquad (22)$$

Then, the Eq. (20) can be rewritten as:

$$W_{BFI} = \sqrt{(S(BFI/BF_c) \frac{BFI}{BF_c} W_{BF_C})^2 + (S(BFI/RO_c) \frac{BFI}{RO_c} W_{RO_C})^2} \qquad (23)$$

where W_{BFI}, $W_{BFC,}$ and W_{ROC} are the same type of uncertainty values for BFI, BF_C, and RO_C, respectively. For instance, W_{BFI} is the uncertainty in BFI at the 95% confidence interval, W_{BFC} is the standard deviation of the highest 1% of measured conductivity

multiplied by the t-value (α=0.05; two-tail) from the Student's distribution, W_{ROC} is the standard deviation of the lowest 1% of measured conductivity multiplied by the t-value (α=0.05; two-tail) from the Student's distribution.

4 Application

4.1 Data and processing

5   The above sensitivity analysis and uncertainty estimation methods were applied to 24 catchments in the United States (Table 1). All basins used in this study are perennial streams, with drainage areas ranging from 10 km^2 to 1258481 km^2. Each gage has about at least 1 year of continuous streamflow and conductivity at the same period. All streamflow and conductivity data are daily average values retrieved from the United States Geological Survey's (USGS) National Water Information System (NWIS) website, http://waterdata.usgs.gov/nwis.

10   The daily baseflow of each basin was calculated using Eq. (1). The 99th percentile of the conductivity of the whole series of streamflow in each basin was used as the BF_C and the 1st percentile as the RO_C. The total baseflow b, the total streamflow y and the baseflow index BFI of each watershed were then calculated. According to the results of the hydrograph separation, the parameter sensitivity indices of BFI for BF_C ($S(BFI/BF_c)$) and RO_C ($S(BFI/RO_c)$) were calculated by Eq. (9) and Eq. (10), respectively.

15   Finally, the uncertainty of f_{bf} in each step was calculated by Eq. (19) and averaged to obtain the Mean W_{fbf} in each basin. The uncertainty (W_{BFI}) of BFI was directly calculated by Eq. (23), and then the values of Mean W_{fbf} and W_{BFI} were compared. For each basin, W_{BFC} is the standard deviation of the highest 1% of measured conductivity multiplied by the t-value (α=0.05; two-tail) from the Student's distribution, W_{ROC} is the standard deviation of the lowest 1% of measured conductivity multiplied by the t-value (α=0.05; two-tail) from the Student's distribution, and W_{QC} is the analytical error in the conductivity (5%) multiplied by

20   the t-value (α=0.05; two-tail).

4.2 Results and discussion

The calculation results are shown in Table 1. The average baseflow index of the 24 watersheds is 0.29, the average sensitivity index of BFI for BF_C ($S(BFI/BF_c)$) is -1.39, and the average sensitivity index of BFI for RO_C ($S(BFI/RO_c)$) is -0.98. The negative sensitivity indices indicate a negative correlation between BFI and BF_C, RO_C. The sensitivity index for BF_C is generally

25   greater than that for RO_C, indicating that BFI is more affected by BF_C (for example, there are 5% uncertainty in both BF_C and RO_C, then BF_C leads to -1.39 times of uncertainty in BFI (-6.95%), while RO_C leads to -0.98 times (4.9%)). Therefore, the determination of BF_C requires more caution, and any small error may lead to greater uncertainty in BFI. Miller et al. (2014) have indicated that anthropogenic activities over long periods of time, or year to year changes in the elevation of the water table may result in temporally changing in the BF_C. He recommended taking different BF_C values per year based on the conductivity values

30   at low flow periods to avoid the effects of BF_C' temporally fluctuations.

Table 1. Basic information, parameter sensitivity analysis, and uncertainty estimation results for 24 basins in the United States. Footnote "a" in the "Area" column indicates that the values are estimated based on data from adjacent sites.

The sensitivity index of BFI for BF_C has a decreasing trend with the increase of time series (n) (Fig. 3(a)) and has an increasing

35   trend with the increase of watershed area (Fig. 3(b)), the correlation coefficients are 0.1698 and 0.4468, respectively. Although the correlations are not obvious, it still has important guiding significance. In the large basin, there are many different subsurface flow paths contributing to stream (Okello et al., 2018), each of which has a unique conductivity value (Miller et al., 2014). It is

difficult to represent the conductivity characteristics of subsurface flow with a special value. Therefore, the conductivity two-component hydrograph separation method has a higher applicability in a small watershed of long time series.

The sensitivity index of BFI for RO_C did not change significantly with the increase of time series and watershed area (Fig. 3(c), Fig. 3(d)). During the rainstorm, the water level of the stream rises sharply, the subsurface flow is suppressed, and the streamflow is almost entirely from the rainfall runoff. At this time, the conductivity of the stream is similar to the conductivity of the local rainfall (Stewart et al., 2007). The electrical conductivity of regional rainfall varies slightly, usually at a fixed value, and has no significant relationship with basin area and year (Munyaneza et al., 2012). Therefore, the temporal and spatial variation characteristics of BFI for RO_C are not obvious.

Figure 3. Scatter plots of sensitivity indices vs. time series (n) and drainage area of the 24 US basins. The watershed area uses a logarithmic axis, while the others are normal axes.

Genereux's method (Eq.19) estimates the average uncertainty of BFI in the 24 basins (Average of Mean W_{fbf}) to be 0.13, whereas the average uncertainty of BFI (Average of W_{BFI}) calculated directly by this paper' method (Eq. 23) is 0.06 (Table 1). Mean W_{fbf} in each basin is generally larger than W_{BFI} (W_{BFI} is about 0.51 times of Mean W_{fbf}), and there is a significant linear correlation (Fig. 4). This shows that the two methods have the same volatility characteristics for BFI uncertainty estimation results, but Genereux's method (Eq. 19) often overestimates the uncertainty of BFI. This also means that when the time series is longer than 365 days (1 year), the measurement errors of conductivity and streamflow will cancel each other and thus reduce the uncertainty of BFI (about half of the original).

Figure 4. Scatter plot of uncertainty in BFI (W_{BFI}) and mean uncertainty in f_{bf} (Mean W_{fbf}).

5 Conclusions

Equation (9) and Eq. (10) can well calculate the sensitivity indices of BFI for BF_C and RO_C. Eq. (23) can estimate the uncertainty of BFI when the time series is larger than 365 days, taking into account the mutual cancellation of conductivity measurement errors. Applications in 24 basins in the United States showed that BFI is more sensitive to BF_C, and future studies should devote more effort to determining the value of BF_C. In addition, the conductivity two-component hydrograph separation method may be more suitable for the long time series in a small watershed.

When the time series is greater than 365 days, the measurement errors of conductivity and streamflow have obvious mutual offset, and its influence on BFI can be neglected. After considering the mutual offset of random errors, the uncertainty of BFI will be reduced to half.

The above conclusions are only from the average of the 24 basins in the United States, and further research is needed in other countries or in more watersheds. The research in this paper only focuses on the two-component hydrograph separation method with conductivity as a tracer, but the parameter sensitivity analysis and uncertainty analysis method of other tracers are very similar to this paper, and it is easy to derive similar equations.

Appendix A

Calculation of the partial derivatives

$$\frac{\partial b_k}{\partial BF_c} = \frac{\partial}{\partial BF_c} \frac{y_k(Q_{ck}-RO_c)}{BF_c-RO_c} = y_k(Q_{ck}-RO_c)\frac{\partial}{\partial BF_c}\frac{1}{BF_c-RO_c} = -y_k\frac{Q_{ck}-RO_c}{(BF_c-RO_c)^2} \tag{A1}$$

$$\frac{\partial b_k}{\partial RO_c} = \frac{\partial}{\partial RO_c} \frac{y_k(Q_{ck}-RO_c)}{BF_c-RO_c} = y_k \frac{\partial}{\partial RO_c} \frac{Q_{ck}-RO_c}{BF_c-RO_c} = y_k \frac{-(BF_c-RO_c)+(Q_{ck}-RO_c)}{(BF_c-RO_c)^2} = y_k \frac{Q_{ck}-BF_c}{(BF_c-RO_c)^2} \tag{A2}$$

$$\frac{\partial BFI}{\partial BF_c} = \frac{\partial}{\partial BF_c} \frac{b}{y} = \frac{1}{y}\sum_{k=1}^{n} \frac{\partial b_k}{\partial BF_c} = \frac{1}{y}\sum_{k=1}^{n}\left(-y_k \frac{Q_{ck}-RO_c}{(BF_c-RO_c)^2}\right)(\text{see Eq. A1}) = \frac{1}{y(BF_c-RO_c)^2}\sum_{k=1}^{n}(y_k RO_c - y_k Q_{ck}) = \frac{yRO_c - \sum_{k=1}^{n}y_k Q_{ck}}{y(BF_c-RO_c)^2} \tag{A3}$$

$$\frac{\partial BFI}{\partial RO_c} = \frac{\partial}{\partial RO_c} \frac{b}{y} = \frac{1}{y}\sum_{k=1}^{n} \frac{\partial b_k}{\partial RO_c} = \frac{1}{y}\sum_{k=1}^{n}\left(y_k \frac{Q_{ck}-BF_c}{(BF_c-RO_c)^2}\right)(\text{see Eq. A2}) = \frac{1}{y(BF_c-RO_c)^2}\sum_{k=1}^{n}(y_k Q_{ck}-y_k BF_c) = \frac{\sum_{k=1}^{n}y_k Q_{ck}-yBF_c}{y(BF_c-RO_c)^2} \tag{A4}$$

$$\frac{\partial b_k}{\partial Q_{ck}} = \frac{\partial}{\partial Q_{ck}} \frac{y_k(Q_{ck}-RO_c)}{BF_c-RO_c} = \frac{1}{BF_c-RO_c} \frac{\partial}{\partial Q_{ck}} y_k(Q_{ck}-RO_c) = \frac{y_k}{BF_c-RO_c} \tag{A5}$$

$$\frac{\partial b_k}{\partial y_k} = \frac{\partial}{\partial y_k} \frac{y_k(Q_{ck}-RO_c)}{BF_c-RO_c} = \frac{(Q_{ck}-RO_c)}{BF_c-RO_c} \frac{\partial}{\partial y_k} y_k = \frac{Q_{ck}-RO_c}{BF_c-RO_c} \tag{A6}$$

$$\frac{\partial BFI}{\partial Q_{ck}} = \frac{\partial}{\partial Q_{ck}} \frac{b}{y} = \frac{1}{y}\sum_{k=1}^{n} \frac{\partial b_k}{\partial Q_{ck}} = \frac{1}{y}\sum_{k=1}^{n} \frac{y_k}{BF_c-RO_c}(\text{see Eq. A5}) = \frac{1}{y(BF_c-RO_c)}\sum_{k=1}^{n} y_k = \frac{1}{BF_c-RO_c} \tag{A7}$$

$$\frac{\partial BFI}{\partial y_k} = \frac{\partial}{\partial y_k} \frac{b}{y} = \frac{\partial}{\partial y_k} \frac{\sum_{k=1}^{n}b_k}{\sum_{k=1}^{n}y_k} = \frac{(\sum_{k=1}^{n}b_k)'(\sum_{k=1}^{n}y_k)-(\sum_{k=1}^{n}b_k)(\sum_{k=1}^{n}y_k)'}{(\sum_{k=1}^{n}y_k)^2} = \frac{y(\sum_{k=1}^{n}b_k)'-b(\sum_{k=1}^{n}y_k)'}{y^2} = \frac{y\sum_{k=1}^{n}(\frac{Q_{ck}-RO_c}{BF_c-RO_c})-b}{y^2}(\text{see Eq. A6}) =$$

$$\frac{y\sum_{k=1}^{n}(Q_{ck}-RO_c)-b(BF_c-RO_c)}{y^2(BF_c-RO_c)} = \frac{\sum_{k=1}^{n}(Q_{ck}-RO_c)-BFI(BF_c-RO_c)}{y(BF_c-RO_c)} \tag{A8}$$

Appendix B

Calculation of the sensitivity indices

$$S(BFI/BF_c) = \frac{\Delta_{BF_c}BFI}{BFI}\Big/\frac{\Delta BF_c}{BF_c} = \frac{yRO_c-\sum_{k=1}^{n}y_k Q_{ck}}{y(BF_c-RO_c)^2}\Delta BF_c \frac{BF_c}{BFI\Delta BF_c}(\text{see Eq. 7}) = \frac{BF_c(yRO_c-\sum_{k=1}^{n}y_k Q_{ck})}{yBFI(BF_c-RO_c)^2} \tag{B1}$$

$$S(BFI/RO_c) = \frac{\Delta_{RO_c}BFI}{BFI}\Big/\frac{\Delta RO_c}{RO_c} = \frac{\sum_{k=1}^{n}y_k Q_{ck}-yBF_c}{y(BF_c-RO_c)^2}\Delta RO_c \frac{RO_c}{BFI\Delta RO_c}(\text{see Eq. 8}) = \frac{RO_c(\sum_{k=1}^{n}y_k Q_{ck}-yBF_c)}{yBFI(BF_c-RO_c)^2} \tag{B2}$$

Appendix C

Prove that $\partial BFI/\partial y_k$ is far less than 1

$$\frac{\partial BFI}{\partial y_k} = \frac{\sum_{k=1}^{n}(Q_{ck}-RO_c)-BFI(BF_c-RO_c)}{y(BF_c-RO_c)}(\text{see Eq. A8}) \tag{C1}$$

Because of BFI>0, $(BF_c-RO_c)>0$, the above formula can be simplified:

$$\frac{\partial BFI}{\partial y_k} < \frac{\sum_{k=1}^{n}(Q_{ck}-RO_c)}{y(BF_c-RO_c)} \tag{C2}$$

Since BF_c is usually much larger than Q_{ck}, the above formula can be rewritten as:

$$\frac{\partial BFI}{\partial y_k} < \frac{\sum_{k=1}^{n}(BF_c-RO_c)}{y(BF_c-RO_c)} = \frac{n(BF_c-RO_c)}{y(BF_c-RO_c)} = \frac{n}{y} = \frac{1}{\bar{y}} \tag{C3}$$

The daily average streamflow ($\bar{y}$) is usually much larger than 1 m^3/d, so $\partial BFI/\partial y_k$ is far less than 1.

Data availability

All streamflow and conductivity data can be retrieved from the United States Geological Survey's (USGS) National Water Information System (NWIS) website use the special gage number, http://waterdata.usgs.gov/nwis.

References

Cartwright, I., Gilfedder, B., and Hofmann, H.: Contrasts between estimates of baseflow help discern multiple sources of water contributing to rivers, Hydrol. Earth Syst. Sci., 18, 15-30, doi:10.5194/hess-18-15-2014, 2014.

15   Costelloe, J. F., Peterson, T. J., Halbert, K., Western, A. W., and McDonnell, J. J.: Groundwater surface mapping informs sources of catchment baseflow, Hydrol. Earth Syst. Sci., 19, 1599-1613, doi:10.5194/hess-19-1599-2015, 2015.

Eckhardt, K.: How to construct recursive digital filters for baseflow separation, Hydrol. Process., 19, 507-515, doi:10.1002/hyp.5675, 2005.

Eckhardt, K.: Technical Note: Analytical sensitivity analysis of a two parameter recursive digital baseflow separation filter,

20   Hydrol. Earth Syst. Sci., 16, 451-455, doi:10.5194/hess-16-451-2012, 2012.

Genereux, D.: Quantifying uncertainty in tracer-based hydrograph separations, Water Resour. Res, 34, 915-919, doi:10.1029/98wr00010, 1998.

Huang, Z. P., Chen, Y. F.: Hydrological statistics, China Water&Power Press, Beijing, China, 2011.

Kline, S. J.: The purposes of uncertainty analysis, J. Fluids Eng., 107, 153-160, 1985.

25   Lott, D. A., Stewart, M. T.: Base flow separation: A comparison of analytical and mass balance methods, J. Hydrol., 535, 525-533, doi:10.1016/j.jhydrol.2016.01.063, 2016.

Mei, Y., Anagnostou, E. N.: A hydrograph separation method based on information from rainfall and runoff records, J. Hydrol., 523, 636-649, doi:10.1016/j.jhydrol.2015.01.083, 2015.

Miller, M. P., Susong, D. D., Shope, C. L., Heilweil, V. M., and Stolp, B. J.: Continuous estimation of baseflow in snowmelt-

30   dominated streams and rivers in the Upper Colorado River Basin: A chemical hydrograph separation approach, Water Resour. Res., 50, 6986–6999, doi:10.1002/2013WR014939, 2014.

Munyaneza, O., Wenninger, J., and Uhlenbrook, S.: Identification of runoff generation processes using hydrometric and tracer methods in a meso-scale catchment in Rwanda, Hydrol. Earth Syst. Sci., 16, 1991-2004, doi:10.5194/hess-16-1991-2012, 2012.

Okello, A. M. L. S., Uhlenbrook, S., Jewitt, G. P. W., Masih, L., Riddell, E. S., and Zaag, P.V.: Hydrograph separation using

35   tracers and digital filters to quantify runoff components in a semi-arid mesoscale catchment, Hydrol. Process., 32, 1334-1350, doi:10.1002/hyp.11491, 2018.

Stewart, M., Cimino, J., and Rorr, M.: Calibration of base flow separation methods with streamflow conductivity, Ground Water, 45, 17-27, doi:10.1111/j.1745-6584.2006.00263.x, 2007.

Taylor, J. R.: An Introduction to Error Analysis: The Study of Uncertainties in Physical Measurements, Univ. Sci. Books, Mill Valley, Calif., 1982.

5   Wagner, R. J., Boulger R. W. Jr., Oblinger, C. J., and Smith, B. A.: Guidelines and standard procedures for continuous water-quality monitors-Station operation, record computation, and data reporting, U.S. Geol. Surv. Tech. Meth., 1-D3, 51 pp, 2006.

Zhang, L. Z.: On the error of hydrologic survey, HoHai University, Nanjing, China, 2005.

Zhang, J., Zhang, Y., Song, J., and Cheng, L.: Evaluating relative merits of four baseflow separation methods in Eastern Australia, J. Hydrol., 549, 252-263, doi:10.1016/j.jhydrol.2017.04.004, 2017.

10

Tables

Table 1. Basic information, parameter sensitivity analysis, and uncertainty estimation results for 24 basins in the United States. Footnote "a" in the "Area" column indicates that the values are estimated based on data from adjacent sites.

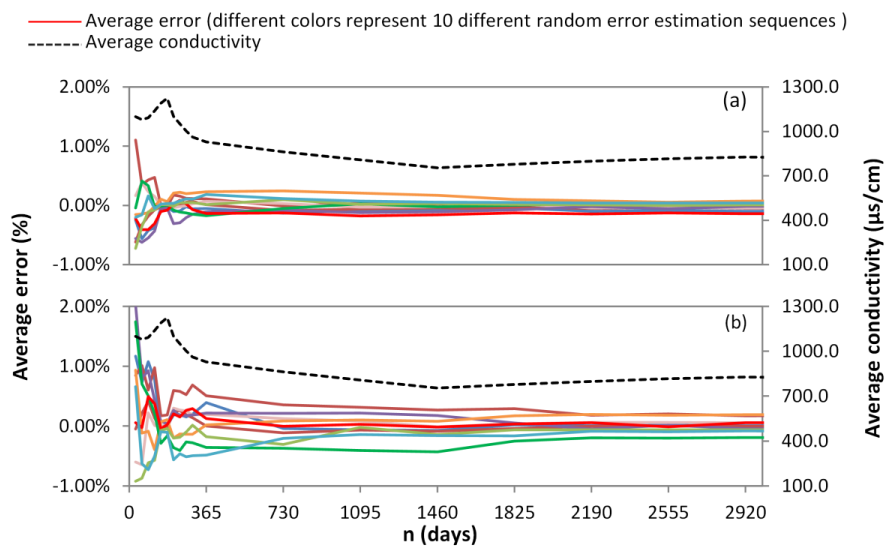| State	Gage Number	N days	Area km²	BF_C µs/cm	RO_C µs/cm	Mean Baseflow m³/s	BFI	$S(BFI/BF_C)$	$S(BFI/RO_C)$	W_{BFI}	Mean W_{fbf}
FL	2298202	1808	966	1190.0	292.5	3.05	0.29	-1.31	-0.78	0.04	0.11
FL	2310545	1218	119[a]	7150.5	531.5	0.10	0.15	-1.09	-0.44	0.05	0.06
FL	2310650	779	77[a]	7195.0	3210.0	0.08	0.45	-1.79	-0.98	0.06	0.14
FL	2303000	728	570	462.0	120.5	3.28	0.30	-1.30	-0.82	0.08	0.17
FL	2298488	1303	76	810.0	194.0	0.20	0.33	-1.30	-0.63	0.05	0.09
FL	2298554	899	207[a]	1155.0	320.5	0.25	0.20	-1.36	-1.55	0.03	0.08
FL	2298492	1478	16	1425.0	304.0	0.04	0.21	-1.26	-1.01	0.03	0.07
FL	2298495	330	10	1905.0	662.0	0.05	0.24	-1.51	-1.66	0.03	0.08
FL	2298527	807	23	1640.0	201.5	0.04	0.14	-1.10	-0.83	0.06	0.16
FL	2298530	1510	17	1520.0	348.0	0.13	0.27	-1.27	-0.80	0.07	0.12
FL	2297100	2979	342	1460.0	221.5	1.54	0.21	-1.17	-0.69	0.04	0.09
FL	2313000	787	4727	449.0	173.0	8.62	0.43	-1.62	-0.84	0.06	0.13
FL	2300500	821	386	470.0	83.0	0.49	0.19	-1.19	-0.90	0.11	0.20
ND	5057000	1401	16757	1520.0	610.0	1.73	0.46	-1.64	-0.81	0.09	0.15
ND	5056000	1277	5361	1770.0	546.0	2.50	0.42	-1.41	-0.61	0.04	0.11
TX	8068275	2801	482	368.0	65.0	4.20	0.15	-1.18	-1.23	0.06	0.13
GA	2336300	1235	225	230.0	63.0	4.00	0.29	-1.36	-0.93	0.24	0.42
GA	2207120	1383	417	381.0	59.0	3.97	0.18	-1.17	-0.86	0.03	0.06
SC	2160105	1363	1966	150.0	51.0	40.27	0.25	-1.49	-1.56	0.03	0.10
SC	2160700	1392	1150	181.0	51.0	24.02	0.26	-1.37	-1.13	0.05	0.11
MO	6894000	1375	477	1110.0	334.0	0.86	0.21	-1.40	-1.59	0.09	0.13
MO	6895500	802	1258481	800.0	428.0	904.39	0.55	-2.14	-0.95	0.05	0.18
ND	5082500	1274	77959	1670.0	427.0	41.48	0.27	-1.33	-0.95	0.06	0.09
KS	7144780	575	1847	1550.0	678.0	0.52	0.44	-1.60	-1.08	0.09	0.17
		Mean					0.29	-1.39	-0.98	0.06	0.13
		Standard deviation (STDEV)					0.11	0.24	0.32	0.04	0.07

5

Figures

Figure 1. Average conductivity error (%) with different distributions along the time series (n), (a) uniform distribution, (b) normal distribution.
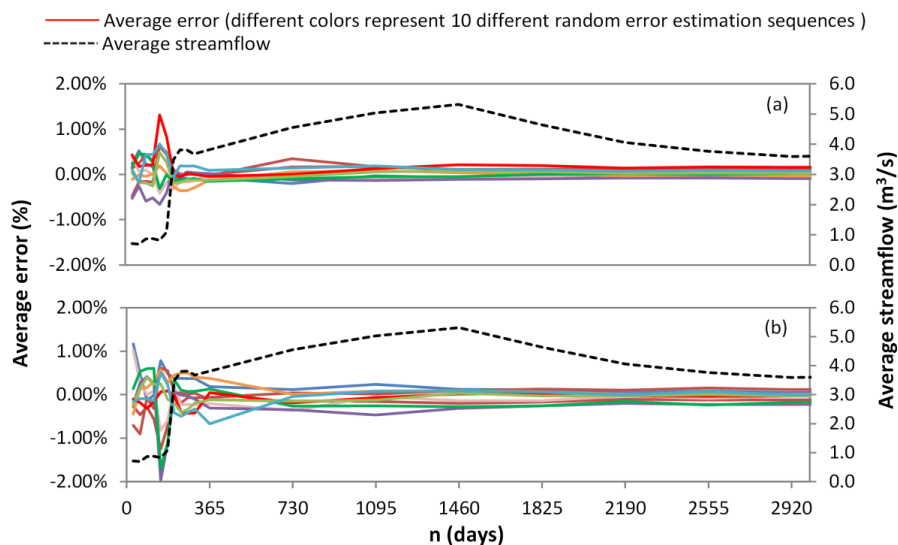
5

Figure 2. Average streamflow error (%) with different distributions along the time series (n), (a) uniform distribution, (b) normal distribution.
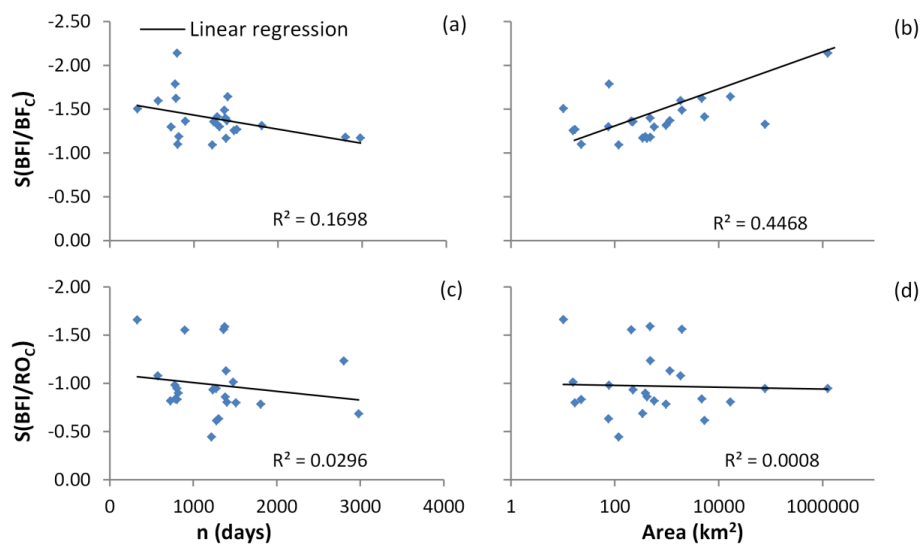
Figure 3. Scatter plots of sensitivity indices vs. time series (n) and drainage area of the 24 US basins. The watershed area uses a logarithmic axis, while the others are normal axes.
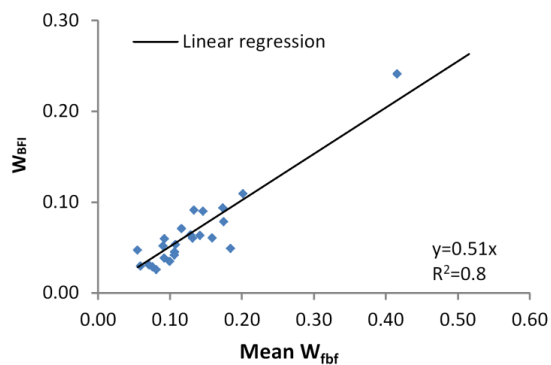
Figure 4. Scatter plot of uncertainty in BFI (W_{BFI}) and mean uncertainty in f_{bf} (Mean W_{fbf}).